Interruption of intrachromosomal looping by CCCTC binding factor decoy proteins abrogates genomic imprinting of human insulin-like growth factor II

He Zhang,[1,2] Beibei Niu,[2] Ji-Fan Hu,[2] Shengfang Ge,[1] Haibo Wang,[1,2] Tao Li,[2] Jianqun Ling,[2] Brandon N. Steelman,[2] Guanxiang Qian,[1] and Andrew R. Hoffman[2]

[1]Department of Biochemistry and Molecular Biology, Ninth People's Hospital, Shanghai Jiaotong University School of Medicine, Shanghai 200025, China
[2]Veterans Affairs Palo Alto Health Care System, Stanford University Medical School, Palo Alto, CA 94304

Monoallelic expression of *IGF2* is regulated by CCCTC binding factor (CTCF) binding to the imprinting control region (ICR) on the maternal allele, with subsequent formation of an intrachromosomal loop to the promoter region. The N-terminal domain of CTCF interacts with SUZ12, part of the polycomb repressive complex-2 (PRC2), to silence the maternal allele. We synthesized decoy CTCF proteins, fusing the CTCF deoxyribonucleic acid–binding zinc finger domain to CpG methyltransferase Sss1 or to enhanced green fluorescent protein. In normal human fibroblasts and breast cancer MCF7 cell lines, the CTCF decoy proteins bound to the unmethylated ICR and to the *IGF2* promoter region but did not interact with SUZ12. EZH2, another part of PRC2, was unable to methylate histone H3-K27 in the *IGF2* promoter region, resulting in reactivation of the imprinted allele. The intrachromosomal loop between the maternal ICR and the *IGF2* promoters was not observed when *IGF2* imprinting was lost. CTCF epigenetically governs allelic gene expression of *IGF2* by orchestrating chromatin loop structures involving PRC2.

Introduction

The transcriptional regulator CCCTC binding factor (CTCF) controls the expression of several genes via chromatin insulation or enhancer blocking (Bell et al., 2001; Ohlsson et al., 2001; Dunn and Davie, 2003; Recillas-Targa et al., 2006). Through the use of different combinations of its 11 highly conserved zinc fingers (ZFs; Mukhopadhyay et al., 2004), CTCF binds to sites within promoters, silencers, and insulators of genes involved in growth, proliferation, differentiation, apoptosis, imprinting, and X chromosome inactivation (Filippova, 2008; Donohoe et al., 2009; Ohlsson et al., 2010). More than 15,000 CTCF binding sites have been identified throughout the genome (Kim et al., 2007). In addition, CTCF has recently been shown to act as a tethering protein, serving as a molecular glue to secure long-range intrachromosomal (Kurukuti et al., 2006; Li et al., 2008) and interchromosomal (Ling et al., 2006) interactions.

CTCF was initially shown to serve as an insulator in the chicken β-globin locus (Bell et al., 1999). The imprinting control region (ICR) of the two coordinately imprinted genes *IGF2* and *H19* was also identified as another CTCF target. The ICR, located in the 5′ flanking region of the *H19* gene and 90 kb downstream of the *Igf2* gene, is maternally unmethylated and paternally methylated (Mann et al., 2000; Reik et al., 2000; Sasaki et al., 2000; Arney, 2003; Engel and Bartolomei, 2003; Murrell et al., 2004) The binding of CTCF to the unmethylated maternal ICR creates a physical boundary, blocking the interaction of downstream enhancers with the remote *IGF2* promoters and silencing the maternal allele (Bell and Felsenfeld, 2000; Hark et al., 2000; Kanduri et al., 2000).

Recent studies have demonstrated that CTCF regulates allelic expression of mouse *Igf2* by forming a long-range intrachromosomal loop (Murrell et al., 2004; Li et al., 2008). This complex intrachromosomal loop is established on the maternal

The Rockefeller University Press $30.00
J. Cell Biol. Vol. 193 No. 3   475–487
www.jcb.org/cgi/doi/10.1083/jcb.201101021

JCB   475

chromosome between the ICR and the *Igf2* promoters, presumably through the formation of CTCF–CTCF dimers or multimers (Yusufzai et al., 2004; Li et al., 2008). CTCF also binds to components of the polycomb repressive complex-2 (PRC2), leading to silencing of the maternal allele through histone K27 methylation (Li et al., 2008), thereby allowing the exclusive expression of *H19* from the maternal allele and *IGF2* from the paternal allele (Mann et al., 2000; Wolffe, 2000; West et al., 2002; Bartolomei, 2003; Engel and Bartolomei, 2003). Biallelic expression of *IGF2* may be seen in many cancer cells, although the molecular basis for this loss of imprinting is poorly understood.

In this work, we extend our examination of the role of CTCF in orchestrating long-distance intrachromosomal looping in the human *IGF2/H19* imprinting domain. We synthesized CTCF decoy proteins that contain the protein's evolutionarily conserved DNA binding domain to decipher the mechanisms through which CTCF controls allelic regulation of human *IGF2*.

Results

CTCF interacts with SUZ12 through its N-terminal (NT) domain

CTCF recruits the PRC2 complex to induce allelic silencing through histone K27 methylation by interacting with SUZ12. We decided to characterize the CTCF domain that interacts with SUZ12. CTCF can be divided into three functional regions: the NT, DNA-binding ZF, and C-terminal (CT) domains. We constructed each domain in a GST vector and purified recombinant proteins using a GST column (Fig. 1 A). Recombinant proteins composed of each domain were incubated with recombinant SUZ12. After pulldown, the GST–protein complexes were separated on a PAGE gel and examined for their interaction with SUZ12 using Western blot analysis. As expected, SUZ12 was detected in the reaction with full-length CTCF (Fig. 1 B, lane 5), confirming the interaction between these two functional proteins as previously reported (Li et al., 2008). SUZ12 bound to the CTCF-NT domain (Fig. 1 B, lane 4), but neither the ZF domain, which is required for DNA recognition and binding, nor the CT domain interacted with SUZ12.

To study the role of the SUZ12 interaction in the maintenance of imprinting, we synthesized a decoy CTCF that maintains the ability to bind target DNA sequences but is unable to interact with SUZ12. For this purpose, the ZF domain was amplified by PCR and was linked in frame to *Sss1* (CpG methyltransferase and ZF-Sss1) or *EGFP* (tracking gene and ZF-EGFP). The addition of Sss1 or EGFP allowed us to synthesize decoy CTCF proteins with a similar molecular mass as that of the full-length CTCF (83-kD native CTCF, 87-kD full-length ZF-Sss1, and 73-kD ZF-EGFP). Sss1 is a DNA methyltransferase that is able to methylate CpG dinucleotides in some DNA sequences near the region where it binds, and EGFP is useful in tracking the transfected cells as a marker. To examine whether the decoy CTCFs interact with SUZ12, the purified recombinant decoy proteins or wild-type CTCF (Fig. 1 C) was incubated with cell extracts, pulled down using Ni–iminodiacetic acid columns, and examined for SUZ12 binding by Western blotting. As expected, SUZ12 was detected in the reaction with full-length

CTCF (Fig. 1 D, top panel, lane 2), but neither ZF-Sss1 nor ZF-EGFP interacted with SUZ12 (Fig. 1 D, top panel, lanes 3 and 4). As controls, full-length CTCF was detected by an antibody that specifically recognizes the NT portion of CTCF (Fig. 1 D, second panel, lane 2), and decoy ZF-EGFP was detected by a GFP antibody (Fig. 1 D, third panel, lane 4).

CTCF decoys compete with endogenous CTCF in binding to the ICR of the *IGF2/H19* domain

The CTCF-Sss1 and CTCF-EGFP genes were packaged into lentiviruses and transduced into human MCF7 (breast cancer), HBF1, and WSF7 (normal fetal skin fibroblasts) cells that maintain normal *IGF2* imprinting, i.e., the exclusive expression from the paternal allele. We used two control cell lines, one with a mock virus carrying the empty vector and one without the virus. The expression of CTCF-Sss1 and CTCF-EGFP was measured by RT-PCR (Fig. 2, A and B) in stable cell clones selected with puromycin. Using EGFP as a tracking marker, we also observed the green fluorescence of the expressed ZF-EGFP fusion protein in MCF7 and WSF7 cells (Fig. 2 C). Using an anti-EGFP antibody, we demonstrated the expression of the predicted fusion protein (Fig. 2 D, lanes 3 and 6), which has a larger molecular weight than the native EGFP control (Fig. 2 D, lanes 2 and 5).

We then used a chromatin immunoprecipitation (ChIP) assay to detect the binding of the fusion proteins to the *IGF2/H19* ICR. Because there are no available antibodies to Sss1, we took an approach in which two antibodies were used to immunoprecipitate different domains of CTCF in ZF-Sss1–transfected cells. The first anti-CTCF antibody that we used specifically recognizes the CT domain of CTCF, which was deleted in the decoy CTCFs; thus, this antibody only detects the binding of the endogenous (native) CTCF. As expected, the ChIP PCR showed that the endogenous CTCF binds to CTCF sites 1 and 3 in human fibroblast HBF1, WSF7, and breast cancer MCF7 cells, in which *IGF2* imprinting is maintained (Fig. 2, E and F, lanes 7 and 8). However, in decoy CTCF-expressing cell clones, no wild-type CTCF binding was detected using an antibody that recognizes the CT domain of CTCF (Fig. 2, E and F, lanes 3 and 4), suggesting that the overexpressed ZF-Sss1 decoy outcompetes the endogenous CTCF for binding at the ICR.

The second antibody specifically recognizes the CTCF ZF domain that is present in both the fusion protein and the endogenous CTCF. ChIP with this antibody showed that the ZF-Sss1 binds to these two CTCF sites (Fig. 2, E and F, lanes 1 and 2).

We also used these two antibodies to examine the CTCF binding to the sixth CTCF site in the ICR region. Again, the data support the finding that the viral overexpressed ZF-Sss1 overrides the endogenous CTCF in binding CTCF site 6 in both MCF7 and HBF1 cells (Fig. 2 G, lanes 1, 2, 5, and 6).

In addition, we also confirmed the direct competition between the ZF-EGFP decoy and the endogenous CTCF by using an anti-EGFP antibody and an antibody against the CT portion of CTCF. As expected, no GFP binding to the ICR sixth CTCF site was detected in normal MCF7 and WSF7 cells (Fig. 2 H, middle panel, lanes 1 and 2). However, in cell clones expressing ZF-EGFP, the decoy directly binds to the ICR in both human
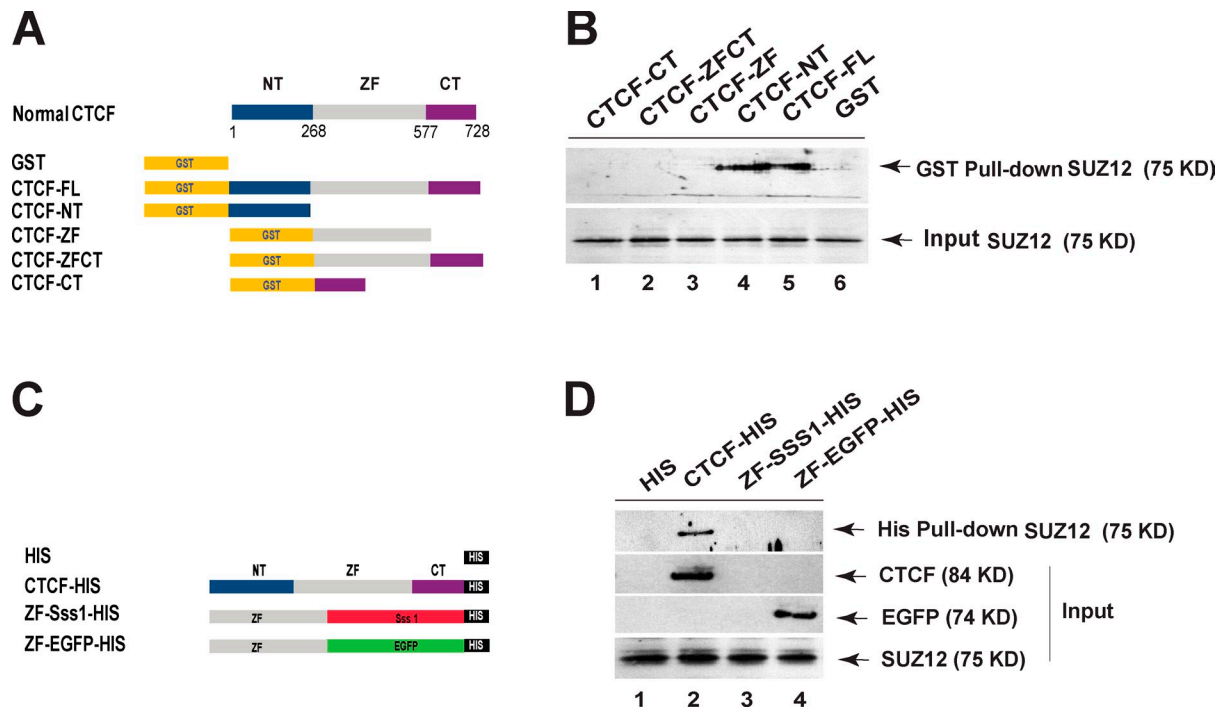
Figure 1. **In vitro binding of recombinant proteins with SUZ12.** (A) A schematic diagram of GST fusion constructs. CTCF-FL, full-length CTCF; NT, N-terminal; ZF, zinc finger domain; CT, C-terminal. (B) Binding of CTCF domains with SUZ12. Input: reaction aliquots collected before the pull-down reaction and analyzed in parallel with the samples using Western blotting with an anti–human SUZ12 antibody. (C) A schematic diagram of His-tagged fusion constructs. CTCF-HIS, His-tagged full-length CTCF; ZF-Sss1-HIS, His-tagged ZF-Sss1; ZF-EGFP-HIS, His-tagged ZF-EGFP. (D) A lack of interaction between His-tagged CTCF decoy proteins and SUZ12. The purified decoy proteins were incubated with cell extracts, and SUZ12 interaction was detected by Western blotting.

fibroblast WSF7 and breast cancer MCF7 cells, as no binding of the native CTCF was detected (Fig. 2 H, lanes 3 and 4). Collectively, these data indicate that the overexpressed decoy proteins outcompete endogenous CTCF in binding to the *IGF2/H19* ICR site.

CTCF binding near the *IGF2* promoters is abolished by decoy CTCF proteins

We then determined where CTCF bound in the *IGF2* promoter region using ChIP. After immunoprecipitation, *IGF2* promoters in the anti-CTCF–precipitated DNA were examined by PCR (Fig. 3 A). In control cells, wild-type CTCF binds to at least three sites in the promoter region (Fig. 3 A, d–f sites, which are near each of the imprinted promoters; and Fig. 3 B, top panel, lanes 10–12), but not to the a site further upstream or the c site between promoter 1 and 2 (Fig. 3 B, top panel, lanes 7 and 9). In the CTCF-Sss1 gene–transfected MCF7 clones, very weak or nonendogenous CTCF binding could be seen in these regions (Fig. 3 B, lanes 2–6). We also detected very weak or non–wild-type CTCF binding near the *IGF2* promoters in CTCF-Sss1–transfected fibroblast HBF1 cells (Fig. 3 C, lanes 2–6). The far upstream a site was included as a control site where Suz12 binds independently without the participation of CTCF (Fig. 3, B and C, lanes 1 and 7).

SUZ12 does not directly bind DNA, but it associates with DNA by interacting with the CTCF in some cell lines (Fig. 1; Li et al., 2008). We examined the recruitment of SUZ12 to the *IGF2* promoters by ChIP analysis and found that SUZ12 interacted in the four *IGF2* promoter regions (Fig. 3 B, second panel, lanes 8 and 10–12). A positive site (a) further upstream was also included, where SUZ12 binding is CTCF independent.

In CTCF-Sss1–expressing cells, however, there was no SUZ12 binding at the *IGF2* promoter region (Fig. 3 B, lanes 2–6), and SUZ12 binding persisted at the control site, a (Fig. 3 B, lanes 1 and 7). These data show that the CTCF-Sss1 protein, which lacks the CTCF NT domain, was unable to bind SUZ12.

Loss of H3-K27 methylation at the *IGF2* promoters

The CTCF-SUZ12 chromosomal interaction is required for specific monoallelic methylation of histone 3 lysine 27 (K27) in *IGF2* promoters (Li et al., 2008). We examined whether the loss of the SUZ12 interaction would affect H3K27 methylation in the *IGF2* promoter region. In control MCF7 cells, we observed H3K27 methylation at the *IGF2* promoters (Fig. 3 B, third panel, lanes 10–12). In contrast, no H3K27 methylation was observed in this region in cells transfected with a CTCF-Sss1 gene (Fig. 3 B, lanes 2–6). We also demonstrated that the CTCF-Sss1 protein abolished the SUZ12 interaction and H3K27 methylation in the *IGF2* promoters in transduced normal human skin fibroblast HBF1 cells (Fig. 3 C).

Interruption of CTCF-mediated intrachromosomal and local looping

We then examined CTCF-mediated intrachromosomal looping using the chromatin conformation capture technique (3C; Dekker et al., 2002; Li et al., 2008). Cloned cells were fixed with 1% formaldehyde, digested with restriction enzyme EcoR1, and then ligated with T4 DNA ligase. In cells in which imprinting is preserved, the *IGF2* promoters directly interact with the
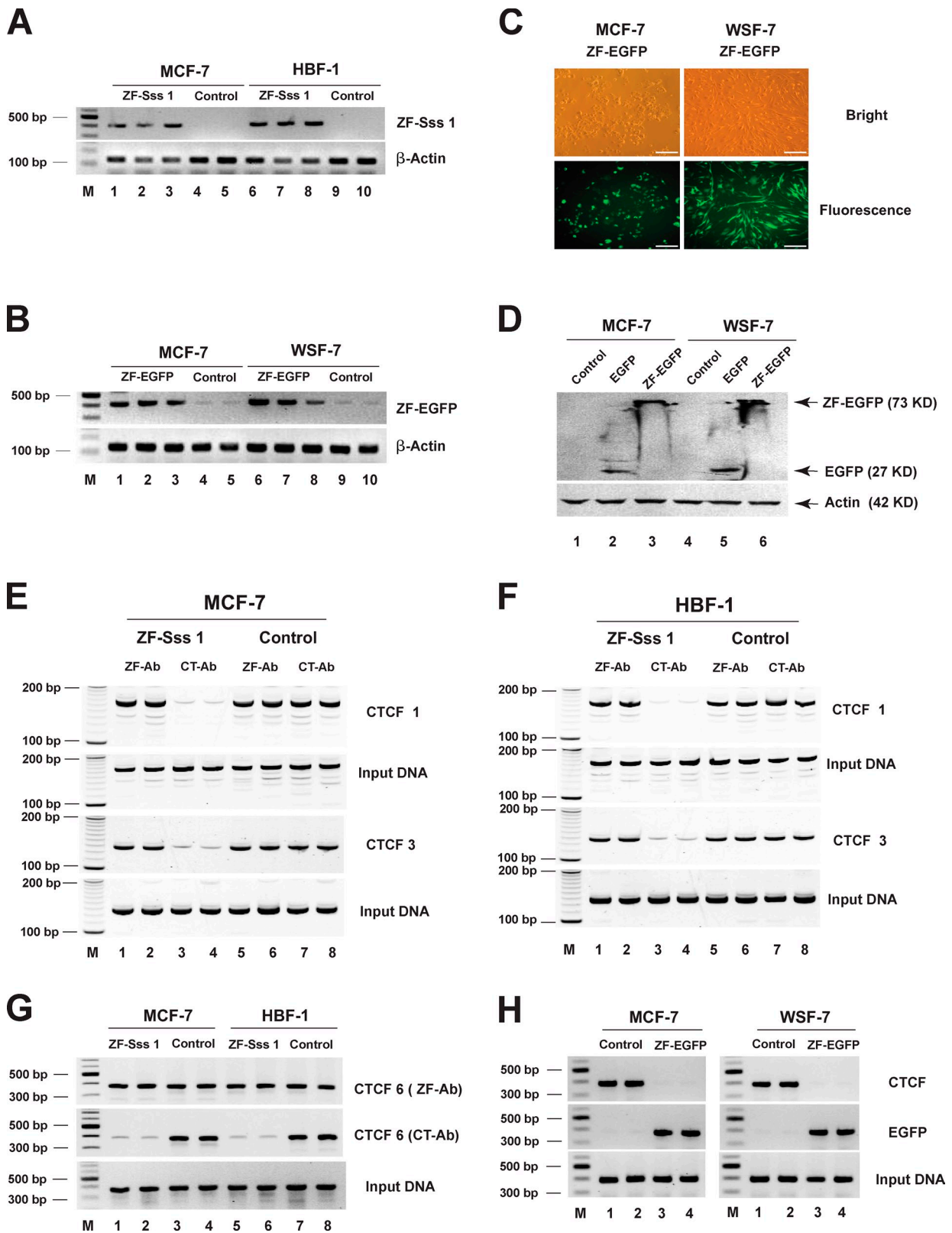
Figure 2. **Overexpression of the decoy CTCF abolishes the *IGF2/H19* ICR binding of the endogenous CTCF.** The expression of decoy CTCF was measured by RT-PCR (A and B), fluorescence microscopy (C), and Western blotting (D). Binding of endogenous CTCF and decoy CTCFs to the ICR was detected by ChIP using two antibodies that recognize the CT and ZF regions of CTCF, respectively (E and F, CTCF sites 1 and 3; and G, CTCF site 6). The competitive binding of native CTCF and ZF-EGFP to the sixth site was detected by a GFP antibody that specifically recognizes the ZF-EGFP and an antibody against the CTCF CT domain (H). Bars, 400 µm.
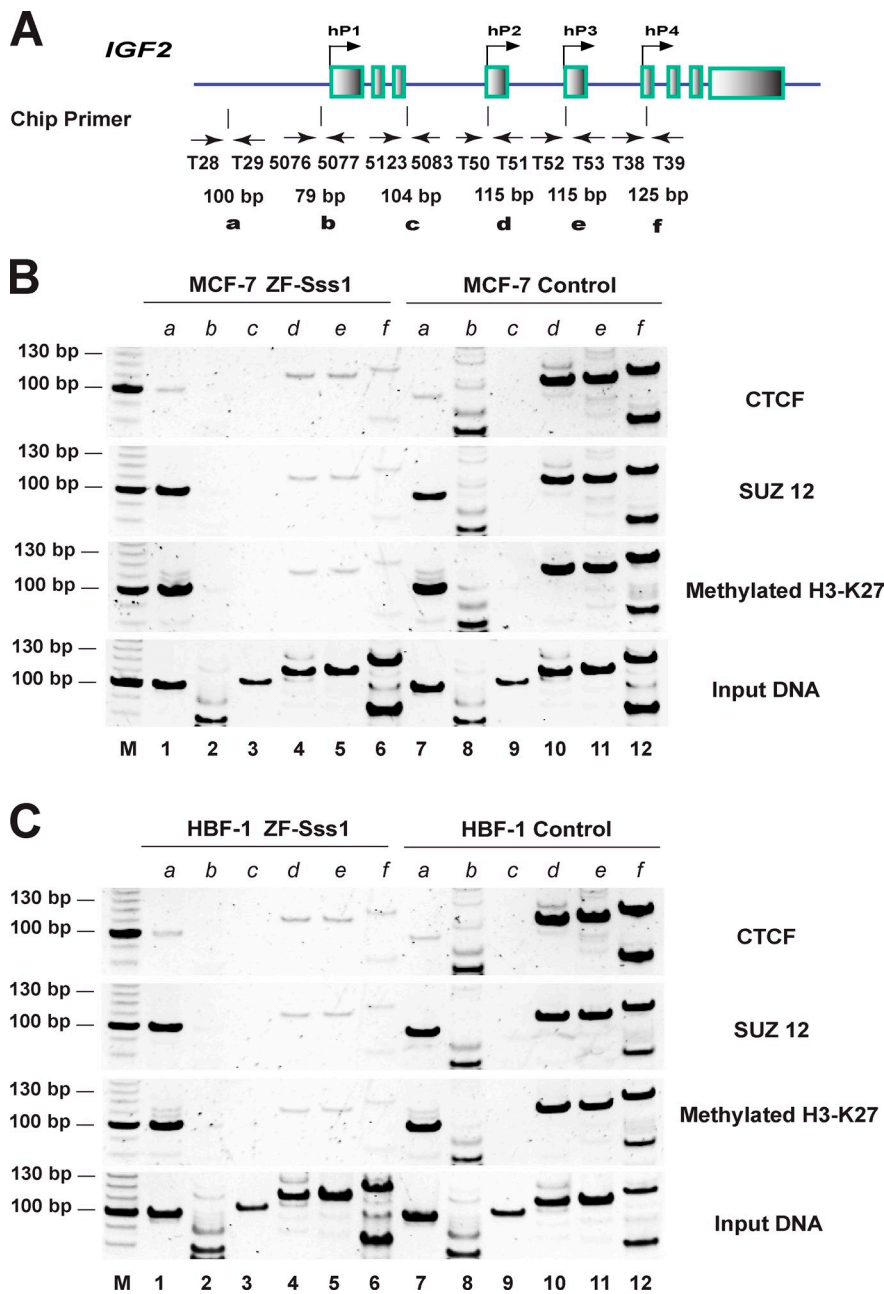
Figure 3. **ChIP assays demonstrating protein binding at the *IGF2* promoter region.** (A) A schematic diagram of the *IGF2/H19* imprinting domain. The exons are depicted as solid boxes. The bottom arrows mark the orientation of ChIP-specific primers. (B and C) Alteration of CTCF binding, SUZ12 interaction, and histone H3-K27 methylation across *IGF2* promoters in decoy CTCF ZF-Sss1–expressing MCF7 breast tumor cells (B) and HBF1 fibroblasts (C). Cross-linked DNA–protein complexes were immunoprecipitated with antiserum against CTCF, SUZ12, or dimethyl-H3-K27 (mK27), followed by PCR amplification with specific primers for the *IGF2* promoters (P1–P4). Input: genomic DNA collected before antibody precipitation.

ICR that is located 80 kb downstream (Fig. 4 A; Li et al., 2008; Vu et al., 2010). Control MCF7 breast cancer cells maintained the intrachromosomal interaction between the *IGF2* promoters and the ICR (Fig. 4 B, lanes 3 and 4). In MCF7 cells that were transfected with the CTCF-Sss1 decoy gene, however, no intrachromosomal interaction was detected between the ICR and the *IGF2* promoters (Fig. 4 B, lanes 1 and 2). The control T48/T49 DNA was detected in all samples. The CTCF-Sss1 decoy protein also interrupted the *IGF2* promoter–ICR intrachromosomal interaction in human skin fibroblasts (Fig. 4 C).

Interestingly, we also noticed changes in the local chromatin structure around the *IGF2* promoters after the expression of the CTCF-Sss1 protein. In control cells, interactions between promoter P2 (1b) and promoter P4 (3b), as well as among 4b, 5b, and 6b (differentially methylated region-2 [DMR2]), were

observed (Fig. 5 A, lanes 3 and 4). In CTCF-Sss1–expressing cells, however, some local chromatin interactions were lost, whereas other new interactions appeared (Fig. 5 A, lanes 1 and 2).

To identify which allele is involved in those lost and new local interactions, we sought two single nucleotide polymorphism sites to distinguish between the parental alleles by endonucleases BfaI and NalIII (Fig. 5, B and C, top). In control cells, the 1b–3b interaction between P2 and P4 was biallelic (Fig. 5 B, lanes 7 and 8). In cells expressing the ZF-Sss1, the new interaction between P2 and P3 was also biallelic (Fig. 5 B, lanes 1 and 2). However, in the DMR2 region, the lost and new interactions were monoallelic (Fig. 5 C, lanes 3–6). These data suggest that CTCF may also be involved in maintaining local chromatin structure around the *IGF2* imprinting locus, although these interactions may not directly participate in the regulation of allelic expression.
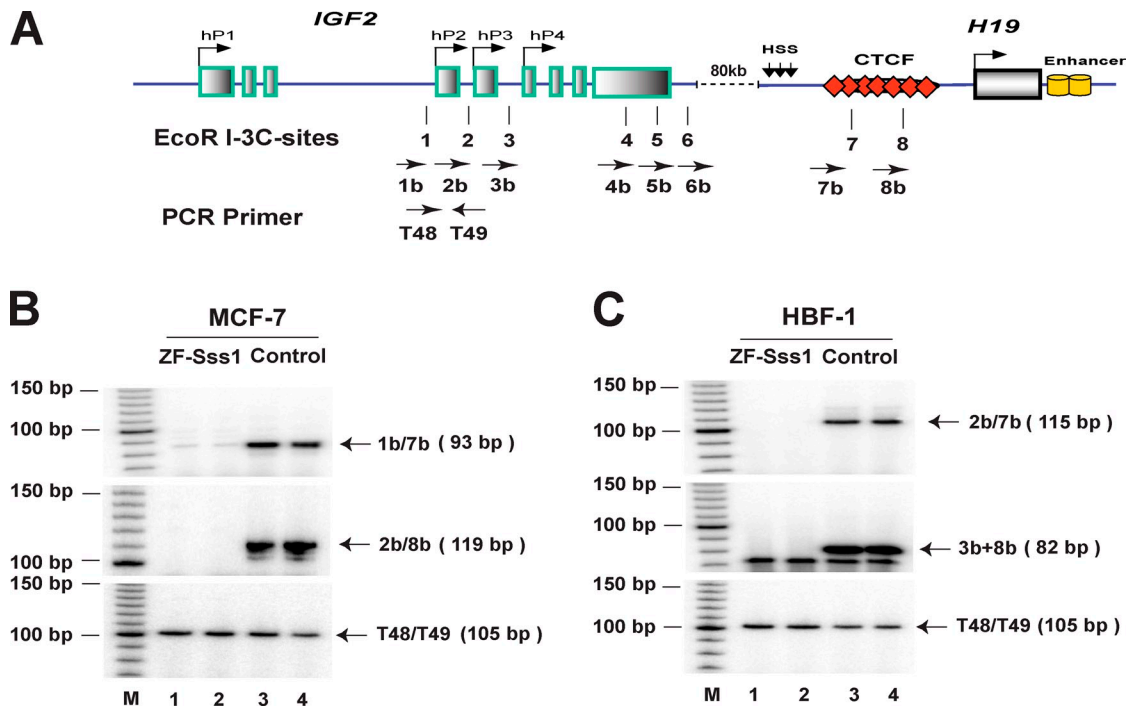
Figure 4. **Intrachromosomal loop between *IGF2* promoters and the ICR.** (A) A schematic diagram of the EcoRI sites in the *IGF2/H19* imprinting locus used for the 3C assay. Arrows under each EcoR1 site mark the orientation of the 3C-specific primers. (B and C) Loss of the long-range intrachromosomal loop between the *IGF2* promoters and the ICR in decoy CTCF–expressing MCF7 cells (B) and human skin fibroblasts (C). ZF-Sss1, Sss1-CTCF–expressing cells; control, wild-type cells.

Aberrant imprinting of *IGF2* by decoy CTCF

We then examined whether allelic expression of *IGF2* was affected in MCF7 and HBF1 cells transfected with CTCF-Sss1. We detected monoallelic expression of *IGF2* in control and mock-treated MCF7 cells (Fig. 6 A, lanes 9–12). In the cells transfected with CTCF-Sss1, *IGF2* became biallelically expressed (Fig. 6 A, lanes 1–6). Similarly, the decoy protein also abolished *IGF2* imprinting in human skin fibroblast cells (Fig. 6 B, lanes 1–6). To confirm the observations, we transduced cells with another CTCF analogue that fuses the CTCF ZF domain with EGFP. This CTCF-EGFP decoy protein also induced biallelic expression of *IGF2* in both MCF7 cells (Fig. 6 C, lanes 1–3). Similar data were also seen in a second human fetal fibroblast cell line, WSF7 (Fig. 6 D, lanes 1–3).

Genomic imprinting of *H19*

In mice, the monoallelic expression of *Igf2* is closely coordinated in a reciprocal fashion with *H19* imprinting through CTCF-ICR insulation (Bartolomei et al., 1993; Bell and Felsenfeld, 2000; Hark et al., 2000). The CTCF insulator marks the boundary in the ICR that is differentially methylated on the two parental alleles. CTCF binds to the unmethylated maternal CTCF DMR and insulates the *Igf2* promoter from the remote enhancer downstream of *H19*. However, allelic methylation of the paternal ICR prevents the binding of CTCF and thus allows the exclusive expression of *H19* from the maternal allele and *Igf2* from the paternal allele (Mann et al., 2000; Wolffe, 2000; West et al., 2002; Bartolomei, 2003; Engel and Bartolomei, 2003). We examined *H19* imprinting in our cell lines and found

that *H19* was biallelically expressed in MCF7 cells transfected with CTCF-Sss1 (Fig. 7 A) and with CTCF-EGFP (Fig. 7 B) but remained monoallelically expressed in human fibroblast HBF1 (Fig. 7 C) and WSF7 (Fig. 7 D) cells. Thus, imprinting of the human *IGF2* and *H19* can be uncoupled in a manner similar to that as observed in human tumors (Feinberg, 1993; Cui et al., 2002; Ulaner et al., 2003; Chen et al., 2006).

Sss1 is a CpG DNA methylase. Using sodium bisulfite sequencing, we did not observe any alteration of DNA methylation at the ICR DNA (Fig. S1). Thus, as reported in human tumors, biallelic *IGF2* expression induced by the decoy protein is not necessarily accompanied by altered DNA methylation in the ICR.

Aberrant *IGF2* and *H19* genomic imprinting affects gene expression

Loss of genomic imprinting is one of the factors that contributes to the increased expression of *IGF2* in some tumors. We thus were interested in whether loss of *IGF2* imprinting induced by decoy CTCFs would alter *IGF2* expression. We quantitated *IGF2* mRNA transcripts by real-time PCR (Fig. 8). *IGF2* is monoallelically expressed in the breast cancer cell line MCF7 and in normal breast tissue. There was increased expression of *IGF2* mRNA in the CTCF decoy–expressing cells, where *IGF2* was biallelically expressed (Fig. 8, A and B). Similarly, loss of *H19* imprinting also led to increased *H19* abundance in MCF7 cells (Fig. 8 A). In normal fibroblasts, where *H19* remained imprinted despite CTCF decoy expression, *H19* gene expression did not increase. We also observed enhanced cell proliferation in human fibroblast cells that show biallelic expression of *IGF2* (Fig. S2). There were no obvious changes in the cell morphology of the infected cells.
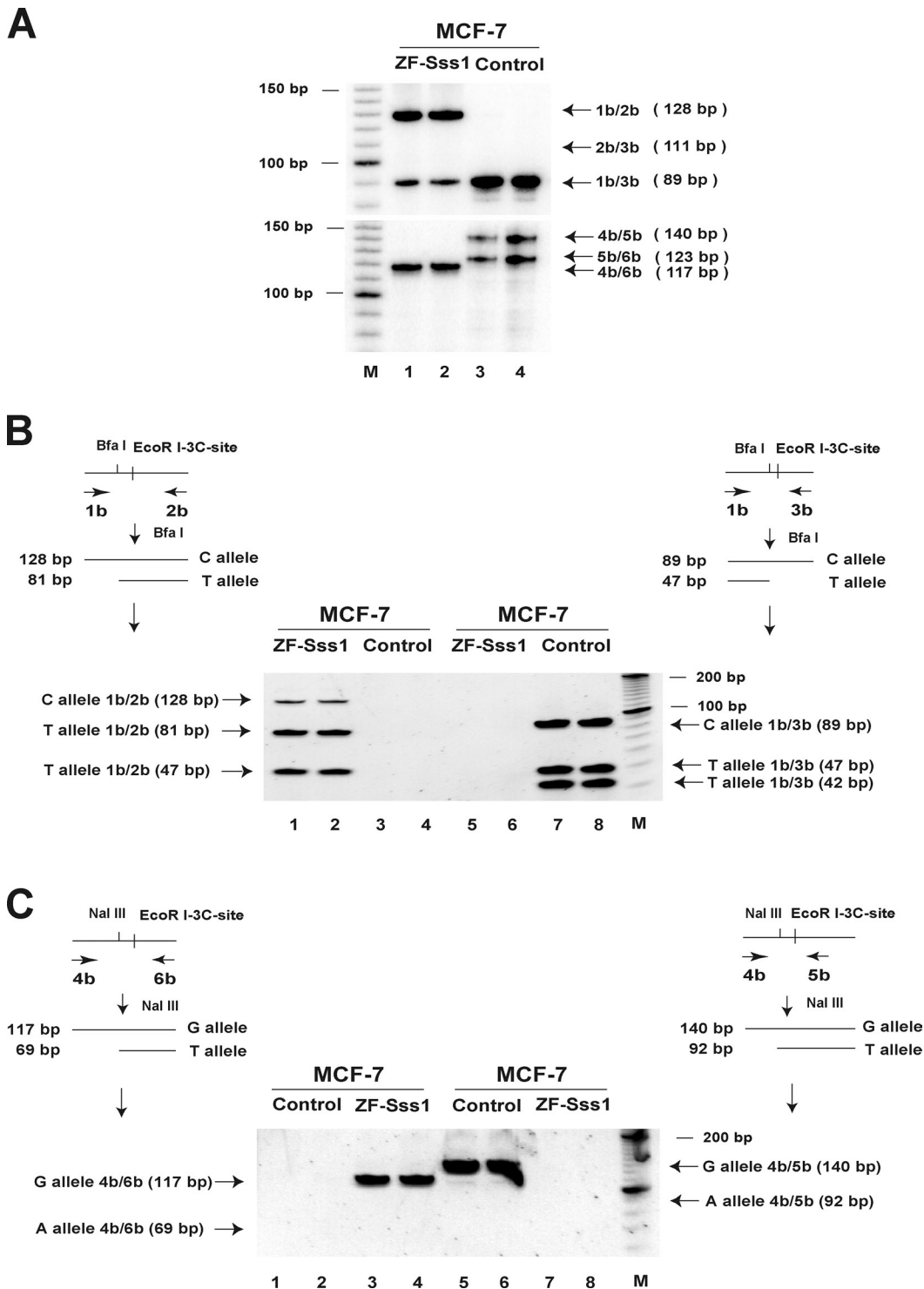
Figure 5. **Allele-specific alteration of local chromatin structure.** (A) Alterations of local chromatin structure in decoy ZF-Sss1–expressing MCF7 cells. (B) Biallelic alteration of local chromatin structure near *IGF2* promoters. After PCR, two parental alleles were distinguished by Bfa1 polymorphic restriction enzyme. (C) Monoallelic alteration of local chromatin structure in the *IGF2* DMR2 region. Two parental alleles were separated by NalIII polymorphic restriction enzyme.

Discussion

In our previous study (Li et al., 2008), we demonstrated that CTCF and Suz12 are coprecipitated from nuclear extracts and interact with each other in a two-hybrid system. RNAi knockdown of Suz12 also leads to reactivation of the maternal *Igf2*

allele and biallelic *Igf2* expression. Our data in this study provide further evidence that CTCF is an active participant in controlling allelic expression of *IGF2* (Fig. 9). CTCF binds to regions around each of the *IGF2* promoters as well as to the unmethylated ICR on the maternal allele. CTCF molecules from these distant loci can dimerize, leading to the formation and

Figure 6. **Loss of *IGF2* imprinting in decoy CTCF–expressing cells.** (A) ZF-Sss1–expressing breast cancer MCF7 cells. (B) ZF-Sss1–expressing human skin fibroblast HBF1. (C) ZF-EGFP–expressing MCF7. (D) ZF-EGFP–expressing human skin fibroblast WSF7 cells. Allelic expression of *IGF2* was determined by polymorphic restriction enzymes AluI (A, C, and D) and ApaI (B). gDNA, genomic DNA as the positive control; mock, empty lentiviral vector that does not contain the decoy constructs; control, untreated cells.
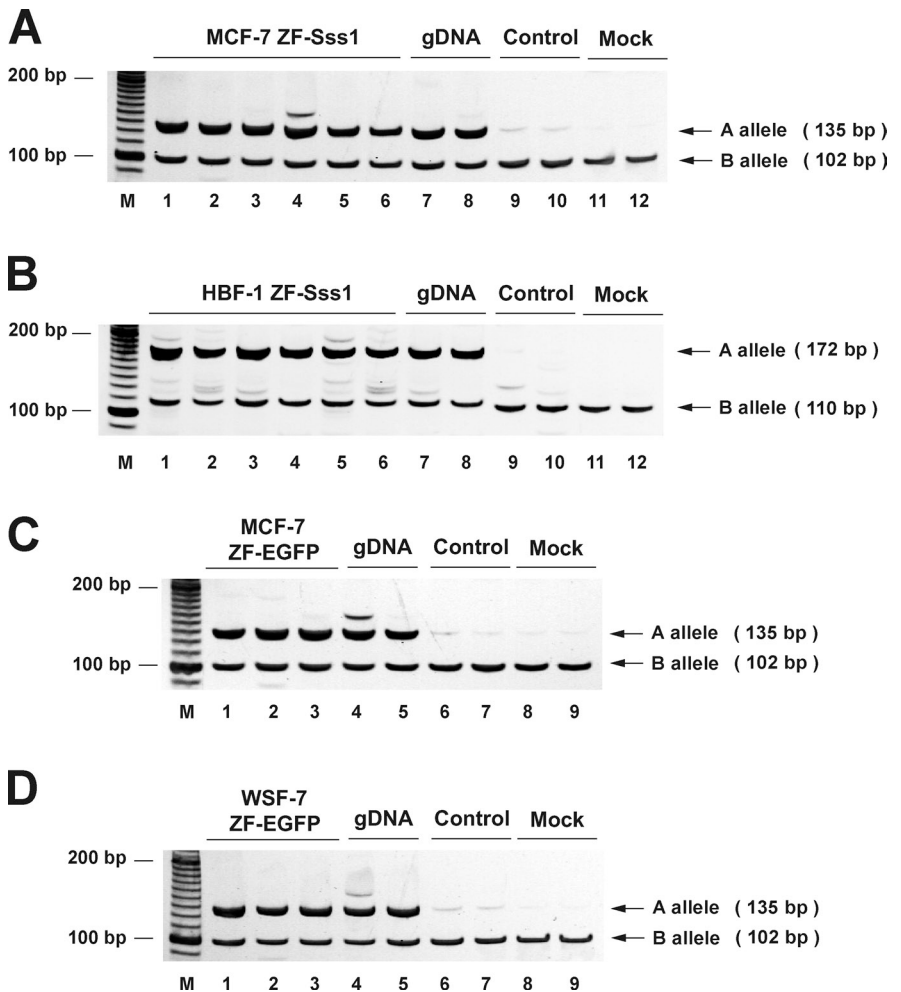
reinforcement of intrachromosomal loops. By orchestrating chromatin loop structures, CTCF serves as a DNA-binding protein scaffold to recruit and bind polycomb repressive complexes and deliver the parent-specific H3K27 methylation signal to the remote *IGF2* promoters, leading to suppression of maternal *IGF2* expression. Through the direct interaction of SUZ12 with the DNA-bound CTCF (Li et al., 2008), the PRC2 complex is recruited specifically to the maternal promoters, where it methylates H3-K27, leading to the formation of a repressive chromatin state on the maternal allele. CTCF cannot bind to the methylated paternal ICR, and, thus, there is no scaffold to secure PRC2 to that site (Bell and Felsenfeld, 2000; Hark et al., 2000). In the absence of CTCF–PRC2 complex binding, a more relaxed chromatin structure is achieved, the paternal *IGF2* promoters are able to access the downstream enhancers, and the gene is transcribed in an allele-specific manner.

CTCF plays a critical role in regulating the allelic expression of *IGF2*. By binding to its target sites at the promoter region and at the distant ICR, CTCF complexes can tether a long-range chromatin loop that delivers the parent-specific methylation signal in the ICR to the remote *IGF2* promoters that do not carry any imprinting marks. Interruption of any components in this pathway, including aberrant ICR DNA methylation, decreased expression of PRC2 proteins, mutation of the ICR, and altered H3-K27 methylation, will cause a loss of *IGF2* imprinting.

Because CTCF regulates many genes by binding to promoters, enhancers, and silencers, it would be of great interest to explore whether CTCF-mediated recruitment of PRC2 proteins is a necessary common mechanism in regulating these targeted genes.

In mouse, *Igf2* and *H19* are tightly coordinated and reciprocally imprinted (Bartolomei et al., 1993) through the CTCF insulating effect on the unmethylated maternal CTCF DMR (Bell and Felsenfeld, 2000; Hark et al., 2000). However, allelic methylation of the paternal ICR abrogates the binding of CTCF and thus allows the exclusive expression of *H19* from the maternal allele and *Igf2* from the paternal allele (Mann et al., 2000; Wolffe, 2000; West et al., 2002; Bartolomei, 2003; Engel and Bartolomei, 2003). Deletion or mutation of the CTCF DMR relaxes the normally silent maternal *Igf2* allele (Thorvaldsen et al., 1998; Srivastava et al., 2000; Szabó et al., 2004). In this study, however, we found that monoallelically expressed *H19* and biallelically expressed *IGF2* coexisted in decoy CTCF–transfected human fibroblast HBF1 and WSF7 cells (Figs. 6 and 7). Thus, in human *IGF2/H19*, the regulation of these two reciprocally imprinted neighboring genes can be uncoupled. This uncoupling has previously been reported in a variety of human tumors (Feinberg, 1993; Cui et al., 2002; Ulaner et al., 2003; Chen et al., 2006).

It should be emphasized that all genetic manipulations, including ICR deletions and/or point mutations in the ICR, designed to prevent CTCF binding, are affected before *Igf2*
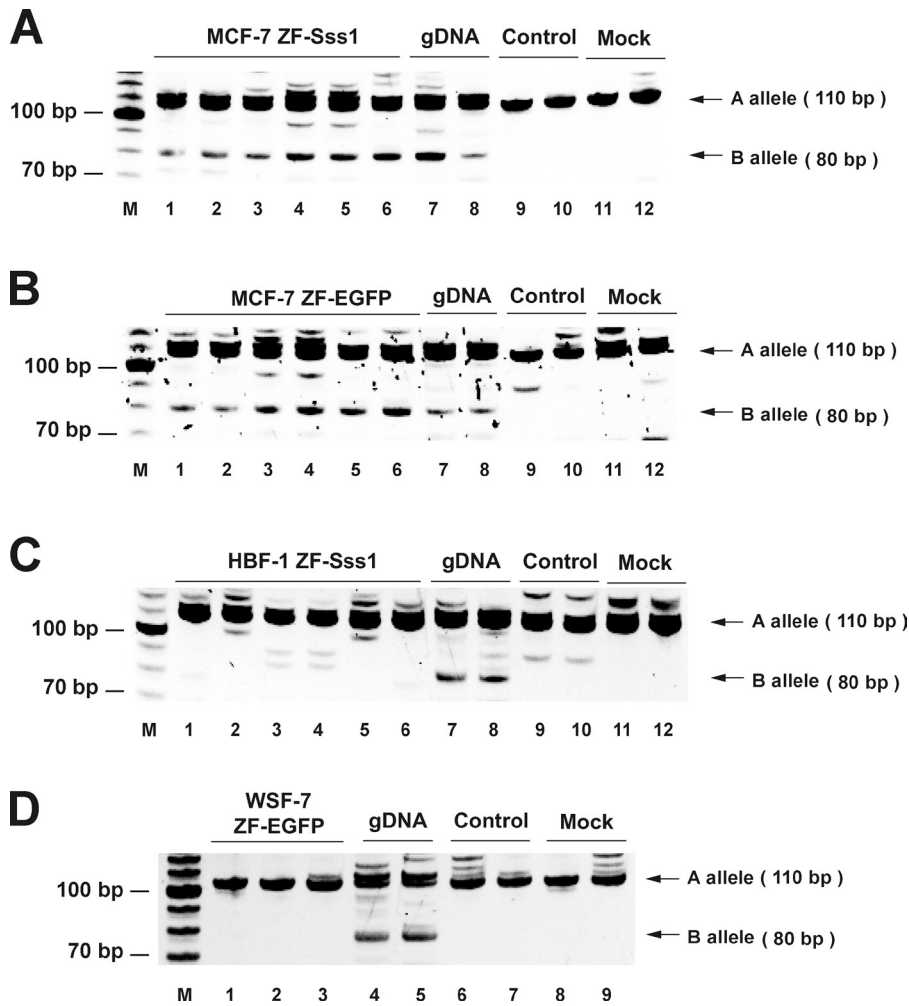
Figure 7. **Decoy proteins induce biallelic expression of *H19* in MCF7 but not in HBF1 or WSF7 cells.** (A–D) The two parental alleles of *H19* were distinguished by polymorphic restriction enzyme Rsa1. Note the biallelic expression of *H19* in MCF7 clones but monoallelic expression of *H19* in HBF1 and WSF7 clones. (B and D) Allelic expression of *H19* in MCF7 (B) and fibroblast WSF7 cells (D) that are stably transfected with ZF-EGFP decoy protein construct. Control, untreated cells; mock, virus carrying the empty vector.

imprinting is set up in early embryos. However, in human tumors, biallelic *IGF2* expression occurs as a result of aberrant regulation of the imprinting maintenance mechanism after imprinting has already been established. In addition, all ICR knockout or mutation experiments have been conducted in mouse models, and the regulation of *IGF2/H19* imprinting may depend on species-specific factors. Thus, the CTCF decoy approach provides an alternative strategy to explore possible mechanisms underlying loss of *IGF2* imprinting in human cells.

The critical involvement of CTCF in maintaining normal monoallelic expression of *IGF2* suggests that the CTCF regulatory pathway may be dysfunctional in human tumors in which *IGF2* is biallelically expressed (Thorvaldsen et al., 1998; Schoenherr et al., 2003; Pant et al., 2004). A maternally transmitted microdeletion of two CTCF binding sites in the ICR results in biallelic *IGF2* expression and *H19* silencing in Beckwith-Wiedemann syndrome (Sparago et al., 2004). Using nuclear transfer, we previously showed that loss of *IGF2* imprinting in human tumor cells was reversed by the imprinting machinery in normal fibroblast cytoplasm, leading to monoallelic expression of *IGF2* in the reconstructed tumor cybrids or hybrids (Chen et al., 2006). Moreover, this epigenetic resetting of *IGF2* imprinting in tumors was not accompanied by any changes in DNA methylation at any of the DMRs (DMR_0, ICR, and K_vDMR_1).

Recently, we also showed that the CTCF-dependent intrachromosomal loop was lost in human fibroblasts in which *IGF2* is biallelically expressed after cycloheximide treatment, despite the fact that DNA methylation in the ICR was not altered (unpublished data).

Similarly, we did not detect any alteration of DNA methylation in the ICR in CTCF-Sss1–transfected MCF7 and HBF1 cells (Fig. S1). Sss1 is a CpG dinucleotide methylase cloned from *Spiroplasma monobiae* strain MQ1 (Renbaum et al., 1990). It de novo methylates DNA exclusively at CpG sites in vivo and in vitro without sequence preference. In a previous study by Xu and Bestor (1997), Sss1 methylase, when fused to the CT domain of the Zif268 ZF domain or a Zif268 derivative that binds to the *p53* binding sites, was able to induce de novo DNA methylation specifically at the target sites. In a parallel study with mouse fibroblasts, we have found that our CTCF-Sss1 construct is able to methylate CTCF binding sites at the K_vDMR_1 in the Kcnq1 imprinting locus (Fitzpatrick et al., 2007), which is ~700 K from mouse *Igf2* (unpublished data). Thus, the gene locus and its local chromatin structure may be critical factors that determine the ability of CTCF-Sss1 to methylate nearby DNA. Alternatively, the methylase, when fused with the ZF domain, may become inactive in this locus by an unknown protection mechanism. Collectively, these findings suggest that, unlike
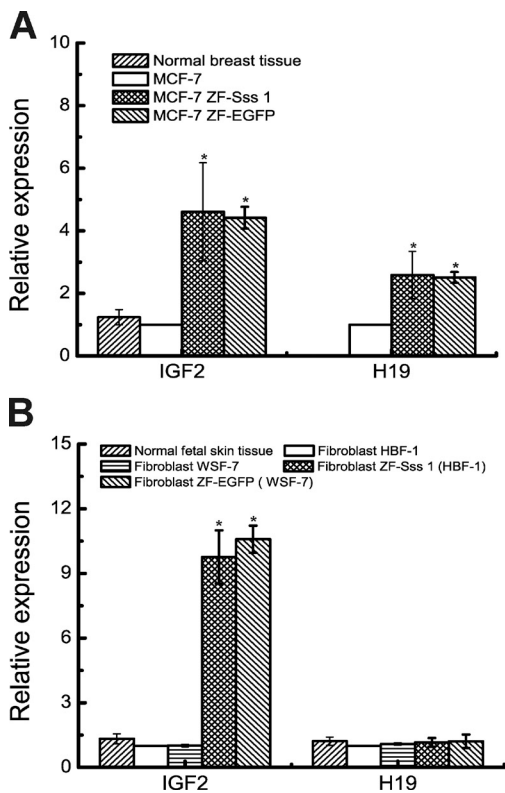
Figure 8. **Real-time PCR quantitation of *IGF2* and *H19* mRNA transcripts.** *IGF2*, *H19*, and the housekeeping *β-actin* genes were coamplified from each cDNA synthesized from normal tissue (human breast and skin), control, and decoy CTCF–expressing cells in MCF7 (A), HBF1, and WSF7 cells (B). *IGF2* and *H19* were quantitated in duplicate for each sample and were determined by a ΔCT and Δ−ΔCT calculation with reference to human *β-actin* gene control. *IGF2* and *H19* expression was normalized and presented as the number by using the *IGF2* and *H19* level in controls (white) as 1 (tissue, $n = 6$; control, $n = 6$; treatment, $n = 6$). *, $P < 0.05$ relative to *IGF2* and *H19* expression in the MCF7 control (A) and fibroblast control (B). All data are presented as means ± SD of three independent experiments.

the mouse *Igf2*, loss of *IGF2* imprinting in tumors may not necessarily be accompanied by changes in DNA methylation in known ICRs, but rather may be related to dysfunction of any of the components of the regulatory network, including the intrachromosomal loop, the ICR, CTCF, or the PRC2 complex. In support of this hypothesis, it is known that human tumors often show a lack of correlation between DNA methylation and *IGF2* imprinting status (Moore et al., 1997; Sullivan et al., 1999; Cui et al., 2002; Chen et al., 2006).

It also should be noted that CTCF regulates many genes by binding to promoters, enhancers, and silencers. The CTCF–PRC2 complex may play a role in the regulation of many other genes that are regulated by CTCF, such as c-myc, β-globin, amyloid β-protein precursor, and X-inactivated genes. Furthermore, CTCF has been described as the master weaver of the genome, facilitating intrachromosomal as well as interchromosomal interactions (Phillips and Corces, 2009). For example, CTCF mediates an interchromosomal colocalization between the *Igf2/H19* ICR on mouse chromosome 7 and *Wsb1/Nf1* on mouse chromosome 11 (Ling et al., 2006). Thus, it would be of great interest to learn whether decoy CTCF proteins alter interchromosomal

associations and, in addition, the expression of these CTCF-regulated genes. Furthermore, the model as described in Fig. 9 does not explain the involvement of the *H19* enhancer. Further studies are needed to delineate how the enhancer is coordinated with the CTCF–Suz12–RPC2 complex in regulating allelic expression of *IGF2*.

Materials and methods

GST-CTCF constructs
To construct recombinant GST fusion proteins, the various CTCF cDNA fragments (full-length CTCF, CTCF-NT, CTCF-ZF, CTCF-ZFCT, and CTCF-CT) were generated from template pOBT7-CTCF vector by PCR amplification containing BamHI–XhoI restriction enzyme (Table S1) using *pfu* polymerase (Agilent Technologies) and were cloned into pGEX-4T-2 vector (Invitrogen). The PET-24b-SUZ12 construct was generated by cloning the full-length SUZ12 cDNA with SalI–NotI site digested from pCMV-SPORT6 (Invitrogen) into pET-24b vector.

CTCF fusion protein construction
The SssI DNA methyltransferase DNA was amplified from the genomic DNA of *S. monobiae* strain MQ1 (33825; American Type Culture Collection). To enhance translation in mammalian cells, four TGA codons that encode tryptophan residing in the *S. monobiae* were converted into TGG by PCR ligation. The cDNA fragment encoding the CTCF ZF domain was generated from the pOBT7-CTCF vector by PCR amplification. These two DNA fragments were then linked by SV40 NLS and a short linker sequence to produce the ZF-Sss1 construct, which was then cloned into the NheI–BamH sites in pCDH-CMV-MCS-EF1-Puro lentivirus vector (SBI). EGFP was amplified from EGFP-N1 vector (Takara Bio Inc.) and was used to replace Sss1 to generate pN1-CTCF ZF-EGFP construct (Table S2).

Recombinant His-tagged constructs
To construct recombinant His-tagged fusion proteins, the full-length CTCF and decoy CTCF (ZF-Sss1 and ZF-EGFP) fragments with NheI and NotI sites were generated from template pOBT7-CTCF vector pCDH-ZF-Sss1 and pCDH-ZF-EGFP by PCR, respectively. These fragments were then cloned into pET-24b vector by framing with His to generate His-tagged fusion proteins (Table S3).

Protein interaction in vitro
All recombinant GST fusion, His-tagged, and SUZ12 proteins were expressed in KRX *Escherichia coli* strain according to the manufacturer's protocol (Li et al., 2008). In brief, purified GST fusion and His-tagged proteins (10 µg) were incubated with 50 µl of cell-free supernatant containing recombinant SUZ12 in 200 µl of binding buffer (20 mM Tris-HCl, pH 7.5, 100 mM NaCl, 2.5 ng/ml BSA, 10 mM EDTA, 0.1% Triton X-100, 1 mM DTT, and 10% glycerol). After incubation for 3 h at 4°C, the glutathione particles (BD) or His tag isolated beads (Invitrogen) containing the protein complex were pulled down and washed three times. Binding proteins were eluted for Western blotting using anti-SUZ12, anti-CTCF, and anti-GFP antibodies (Abcam).

Lentiviral transduction
The lentiviruses were generated in 293SF-PacLV cells according to the protocol provided by the manufacturer. The viral supernatants were filtered through a 0.45-mm filter, concentrated by the PEG-IT kit (SBI), and aliquoted in a −80°C freezer for long-term storage. Human fibroblasts and tumor cells were seeded at 1.0×10^5 cells per well of a 6-well plate 24 h before transduction. The medium was replaced with virus-containing supernatant containing 5 mg/ml polybrene (Sigma-Aldrich) and incubated overnight. 24 h after transduction, the virus-containing medium was replaced with fresh medium for further culture. 4 d later, the infected cells were harvested by trypsinization and replated on a new 100-mm dish. When cell confluence reached 20–30%, the culture medium was replaced by fresh medium containing 1 µg/ml puromycin for colony selection. The medium was changed every 3–4 d. After selection, colonies were chosen and expanded for further analyses.

Chromosome conformation capture (3C)
The 3C assay was performed as described previously (Dekker et al., 2002; Li et al., 2008). In brief, 1.0×10^7 cells were cross-linked with 2%
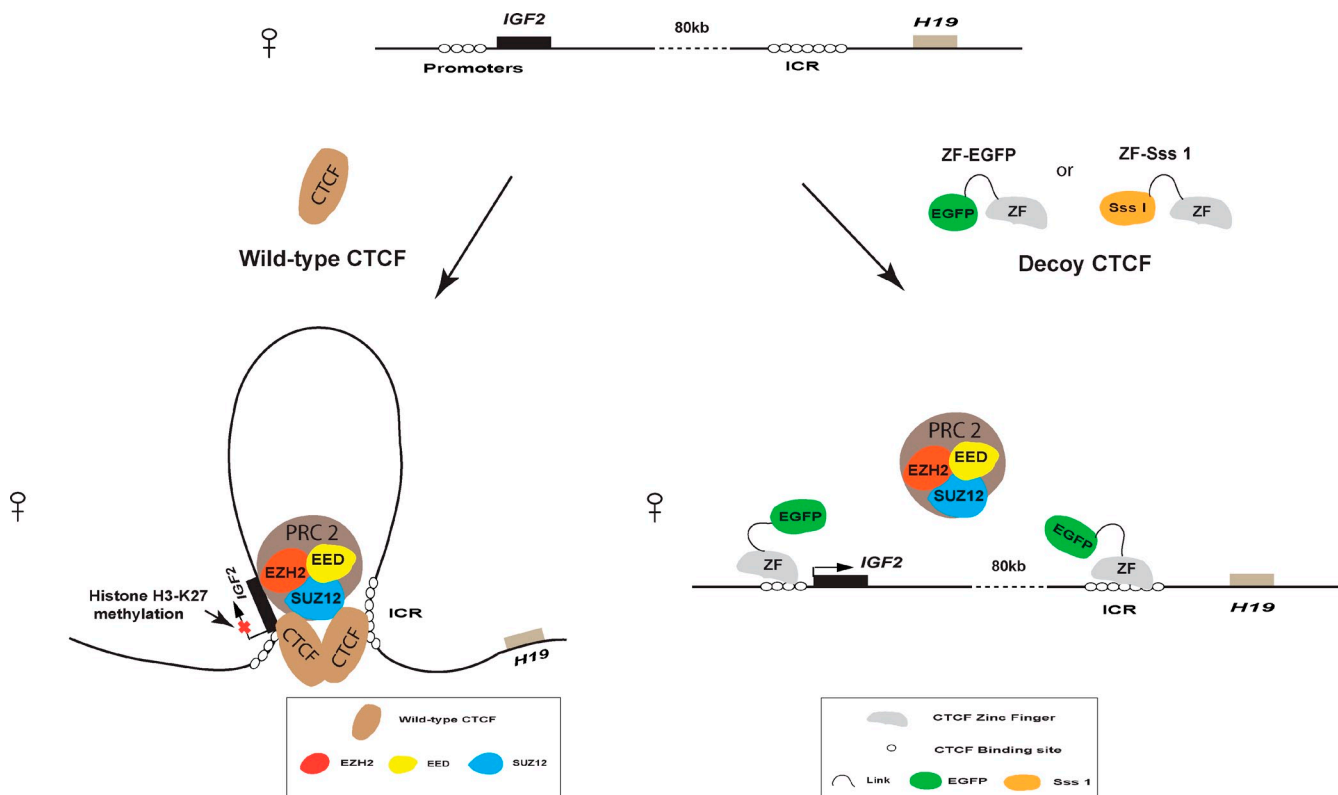
Figure 9. **Model of the *IGF2/H19* imprinting region.** Aberrant *IGF2* imprinting induced by the decoy CTCF. In cells that maintain normal *IGF2* imprinting, CTCF orchestrates an intrachromosomal loop by binding to both the unmethylated ICR and to the *IGF2* promoters on the maternal allele. CTCF then dimerizes, tethering the loop together. CTCF interacts with SUZ12 in PRC2, thereby guiding the K27 methylase EZH2 to the *IGF2* promoters, where it methylates histone H3 and causes the allele-specific suppression of the maternal promoters. When the decoy CTCF binds to the ICR, it fails to recruit SUZ12, thus abrogating the *IGF2* promoters/ICR intrachromosomal loop. Without the CTCF–PRC2 interaction, EZH2 cannot methylate H3-K27 in the *IGF2* promoters, resulting in the reactivation of the normally suppressed maternal allele.

formaldehyde and lysed with cell lysis buffer (10 mM Tris, pH 8.0, 10 mM NaCl, 0.2% NP-40, and protease inhibitors). Nuclei were collected, suspended in 1× restriction enzyme buffer in the presence of 0.3% SDS, and incubated at 37°C for 1 h. Triton X-100 was then added to a final concentration of 1.8% to sequester the SDS. An aliquot of nuclei (2 × 10^6) was digested with 800 U of restriction enzyme EcoRI at 37°C overnight. After stopping the reaction by adding 1.6% SDS and incubating the mixture at 65°C for 20 min, chromatin DNA was diluted with ligation reaction buffer (New England Biolabs, Inc.), and 2 µg DNA was ligated with 4,000 U T4 DNA ligase (New England Biolabs, Inc.) at 16°C for 4 h (final DNA concentration of 2.5 µg/ml). After treatment with 10 mg/ml proteinase K at 65°C overnight to reverse cross-links and with 0.4 µg/ml RNase A for 30 min at 37°C, DNA was extracted with phenol-chloroform, ethanol precipitated, and used for PCR amplification of the ligated DNA products. PCR primers used in this study are listed in Table S4.

ChIP
ChIP assays were performed as described previously (Li et al., 2008). In brief, five million cells were fixed with 1% formaldehyde and sonicated for 180 s (10 s on and 10 s off) on ice with a Branson sonicator with a 2-mm microtip at 40% output control and 90% duty cycle settings. The 1 ml of sonicated chromatin was clarified by centrifugation, aliquoted, and snap frozen in liquid nitrogen. To perform ChIP, 150 µl of sonicated chromatin was diluted 10-fold and purified with 2–5 µl of specific antiserum and 60 µl protein G–agarose. Antibodies to GFP, CTCF, SUZ12, and dimethyl-H3-K27 (lysine 27 of histone H3) were obtained from Abcam. DNA that was released from the bound chromatin after cross-linking reversal and proteinase K treatment was precipitated and diluted in 100 µl of low TE buffer (1 mM Tris and 0.1 mM EDTA). PCR reactions were performed under liquid wax in a reaction containing 1 µl ChIP (or input) DNA, 0.5 µM of appropriate primer pairs, 50 µM deoxynucleotide triphosphate, and 0.2 U Klen-TaqI (Ab Peptides). Standard PCR conditions were 95°C for 2 min followed by 35 cycles of 95°C for 15 s, 65°C for 30 s of annealing, and 72°C for 30 s of extension (Table S5). The PCR products were separated

on a 5% polyacrylamide–urea gel and quantified by a PhosphorImager (Molecular Dynamics).

Examination of *IGF2* and *H19* imprinting
Total RNA was extracted from tissues by TRI-REAGENT (Sigma-Aldrich) according to the manufacturer's guide, and cDNA was synthesized with RNA reverse transcription. Genomic imprinting of *IGF2* was examined by PCR in cDNA samples as previously described using primers specific for two polymorphic restriction enzymes (Apa1 and Alu1) in the last exon of human *IGF2*. After PCR, two parental alleles were distinguished by the digestion of polymorphic restriction enzymes AluI and ApaI and were separated on 5% polyacrylamide gel (Hu et al., 1996, 1997; Chen et al., 2006). Note that in CTCF decoy–expressed cells, the imprinted A allele became activated, leading to biallelic expression of *IGF2*. Allelic expression of *H19* was assessed by polymorphic restriction enzyme Rsa1. PCR primers used to measure allelic expression of *IGF2* and *H19* are listed in Table S6.

Real-time RT-PCR
Quantitative real-time RT-PCR amplification was performed using QuantiTect SYBR green (QIAGEN) as previously described (Chen et al., 2006). Specifically, total RNA was extracted by TRIZOL reagent (Invitrogen), and cDNA was synthesized with RNA reverse transcription. The threshold cycle (Ct) values of *IGF2* and *H19* were quantitated by quantitative PCR in duplicate using a sequence detector (ABI Prism 7900HT; Applied Biosystems) according to the manufacturer's protocol and was normalized over the Ct of the *β-actin* control (Table S7).

DNA methylation analysis
Total nucleic acids extracted from fibroblast and tumor cells were used to examine DNA methylation patterns. As previously described (Ulaner et al., 2003), total nucleic acids were treated with sodium bisulfite, and DNA in the *IGF2/H19* DMR was amplified with DNA methylation-specific primers designed for CTCF binding sites (Table S8). After PCR, methylated and unmethylated DNAs were separated by MluI. To examine the status of DNA

methylation in every CpG site in the key sixth CTCF binding region, the amplified PCR DNAs were cloned into TA vector (Invitrogen) and were sequenced using the vector primer.

Western blot analysis
Protein interaction was determined by Western blotting as previously described. Pull-down protein complexes were separated by SDS-PAGE in 12% (wt/vol) polyacrylamide gels and transferred to polyvinylidene fluoride membranes. Membranes were used in immunoblotting with anti-SUZ12, anti-CTCF, and anti-GFP antibody (Abcam).

Survival assay
Cells were seeded at 5,000 cells per well in flat-bottomed 96-well plates. At the end of the incubation time, 20 µl of 5-mg/ml MTT (3-(4,5-dimethylthiazol-2-yl)-2,5-diphenyltetrazolium bromide; Sigma-Aldrich) in PBS was added to each well. After 4 h, media were discarded, and cells were lysed with 100 µl DMSO. Cells were incubated for a further 30 min at 37°C with gentle shaking. The optical density was determined with a microplate reader at 570 nm. Absorbance values were normalized to the values of control cells at day 1 to calculate the percentage of survival.

Statistical analysis
All experiments were performed in triplicate, and the data were expressed as mean ± SD. The comparative Ct method was applied in the quantitative real-time RT-PCR assay according to the $\Delta-\Delta Ct$ method. The data were analyzed with t test or by one-way analysis of variance, and results were considered statistically significant at $P \leq 0.05$.

Online supplemental material
Fig. S1 shows DNA methylation at the CTCF ICR in the *IGF2/H19* imprinting domain. Fig. S2 shows the growth characteristics of decoy CTCF–expressing cells. Table S1 shows primers used for construction of various GST-CTCF fusion proteins. Table S2 shows primers used for construction of decoy CTCF vectors. Table S3 shows primers used for construction of His-tagged fusion proteins. Table S4 shows primers used for 3C at the *IGF2* locus. Table S5 shows primers used for ChIP assays. Table S6 shows primers used for allelic expression of *IGF2* and *H19* imprinted genes. Table S7 shows primers used for real-time PCR. Table S8 shows primers used for DNA methylation of the sixth CTCF binding site in the ICR of the *IGF2/H19* locus. Online supplemental material is available at http://www.jcb.org/cgi/content/full/jcb.201101021/DC1.

References

Arney, K.L. 2003. *H19* and *Igf2*—enhancing the confusion? *Trends Genet.* 19:17–23. doi:10.1016/S0168-9525(02)00004-5

Bartolomei, M.S. 2003. Epigenetics: role of germ cell imprinting. *Adv. Exp. Med. Biol.* 518:239–245.

Bartolomei, M.S., A.L. Webber, M.E. Brunkow, and S.M. Tilghman. 1993. Epigenetic mechanisms underlying the imprinting of the mouse *H19* gene. *Genes Dev.* 7:1663–1673. doi:10.1101/gad.7.9.1663

Bell, A.C., and G. Felsenfeld. 2000. Methylation of a CTCF-dependent boundary controls imprinted expression of the *Igf2* gene. *Nature*. 405:482–485. doi:10.1038/35013100

Bell, A.C., A.G. West, and G. Felsenfeld. 1999. The protein CTCF is required for the enhancer blocking activity of vertebrate insulators. *Cell*. 98:387–396. doi:10.1016/S0092-8674(00)81967-4

Bell, A.C., A.G. West, and G. Felsenfeld. 2001. Insulators and boundaries: versatile regulatory elements in the eukaryotic genome. *Science*. 291:447–450. doi:10.1126/science.291.5503.447

Chen, H.L., T. Li, X.W. Qiu, J. Wu, J.Q. Ling, Z.H. Sun, W. Wang, W. Chen, A. Hou, T.H. Vu, et al. 2006. Correction of aberrant imprinting of *IGF2*

in human tumors by nuclear transfer-induced epigenetic reprogramming. *EMBO J.* 25:5329–5338. doi:10.1038/sj.emboj.7601399

Cui, H., P. Onyango, S. Brandenburg, Y. Wu, C.L. Hsieh, and A.P. Feinberg. 2002. Loss of imprinting in colorectal cancer linked to hypomethylation of *H19* and *IGF2*. *Cancer Res.* 62:6442–6446.

Dekker, J., K. Rippe, M. Dekker, and N. Kleckner. 2002. Capturing chromosome conformation. *Science*. 295:1306–1311. doi:10.1126/science.1067799

Donohoe, M.E., S.S. Silva, S.F. Pinter, N. Xu, and J.T. Lee. 2009. The pluripotency factor Oct4 interacts with Ctcf and also controls X-chromosome pairing and counting. *Nature*. 460:128–132. doi:10.1038/nature08098

Dunn, K.L., and J.R. Davie. 2003. The many roles of the transcriptional regulator CTCF. *Biochem. Cell Biol.* 81:161–167. doi:10.1139/o03-052

Engel, N., and M.S. Bartolomei. 2003. Mechanisms of insulator function in gene regulation and genomic imprinting. *Int. Rev. Cytol.* 232:89–127. doi:10.1016/S0074-7696(03)32003-0

Feinberg, A.P. 1993. Genomic imprinting and gene activation in cancer. *Nat. Genet.* 4:110–113. doi:10.1038/ng0693-110

Filippova, G.N. 2008. Genetics and epigenetics of the multifunctional protein CTCF. *Curr. Top. Dev. Biol.* 80:337–360. doi:10.1016/S0070-2153(07)80009-3

Fitzpatrick, G.V., E.M. Pugacheva, J.Y. Shin, Z. Abdullaev, Y. Yang, K. Khatod, V.V. Lobanenkov, and M.J. Higgins. 2007. Allele-specific binding of CTCF to the multipartite imprinting control region KvDMR1. *Mol. Cell. Biol.* 27:2636–2647. doi:10.1128/MCB.02036-06

Hark, A.T., C.J. Schoenherr, D.J. Katz, R.S. Ingram, J.M. Levorse, and S.M. Tilghman. 2000. CTCF mediates methylation-sensitive enhancer-blocking activity at the *H19/Igf2* locus. *Nature*. 405:486–489. doi:10.1038/35013106

Hu, J.F., T.H. Vu, and A.R. Hoffman. 1996. Promoter-specific modulation of insulin-like growth factor II genomic imprinting by inhibitors of DNA methylation. *J. Biol. Chem.* 271:18253–18262. doi:10.1074/jbc.271.30.18253

Hu, J.F., T.H. Vu, and A.R. Hoffman. 1997. Genomic deletion of an imprint maintenance element abolishes imprinting of both insulin-like growth factor II and *H19*. *J. Biol. Chem.* 272:20715–20720. doi:10.1074/jbc.272.33.20715

Kanduri, C., V. Pant, D. Loukinov, E. Pugacheva, C.F. Qi, A. Wolffe, R. Ohlsson, and V.V. Lobanenkov. 2000. Functional association of CTCF with the insulator upstream of the *H19* gene is parent of origin-specific and methylation-sensitive. *Curr. Biol.* 10:853–856. doi:10.1016/S0960-9822(00)00597-2

Kim, T.H., Z.K. Abdullaev, A.D. Smith, K.A. Ching, D.I. Loukinov, R.D. Green, M.Q. Zhang, V.V. Lobanenkov, and B. Ren. 2007. Analysis of the vertebrate insulator protein CTCF-binding sites in the human genome. *Cell*. 128:1231–1245. doi:10.1016/j.cell.2006.12.048

Kurukuti, S., V.K. Tiwari, G. Tavoosidana, E. Pugacheva, A. Murrell, Z. Zhao, V. Lobanenkov, W. Reik, and R. Ohlsson. 2006. CTCF binding at the *H19* imprinting control region mediates maternally inherited higher-order chromatin conformation to restrict enhancer access to *Igf2*. *Proc. Natl. Acad. Sci. USA*. 103:10684–10689. doi:10.1073/pnas.0600326103

Li, T., J.F. Hu, X. Qiu, J. Ling, H. Chen, S. Wang, A. Hou, T.H. Vu, and A.R. Hoffman. 2008. CTCF regulates allelic expression of *Igf2* by orchestrating a promoter-polycomb repressive complex 2 intrachromosomal loop. *Mol. Cell. Biol.* 28:6473–6482. doi:10.1128/MCB.00204-08

Ling, J.Q., T. Li, J.F. Hu, T.H. Vu, H.L. Chen, X.W. Qiu, A.M. Cherry, and A.R. Hoffman. 2006. CTCF mediates interchromosomal colocalization between *Igf2/H19* and *Wsb1/Nf1*. *Science*. 312:269–272. doi:10.1126/science.1123191

Mann, J.R., P.E. Szabó, M.R. Reed, and J. Singer-Sam. 2000. Methylated DNA sequences in genomic imprinting. *Crit. Rev. Eukaryot. Gene Expr.* 10:241–257.

Moore, T., M. Constancia, M. Zubair, B. Bailleul, R. Feil, H. Sasaki, and W. Reik. 1997. Multiple imprinted sense and antisense transcripts, differential methylation and tandem repeats in a putative imprinting control region upstream of mouse *Igf2*. *Proc. Natl. Acad. Sci. USA*. 94:12509–12514. doi:10.1073/pnas.94.23.12509

Mukhopadhyay, R., W. Yu, J. Whitehead, J. Xu, M. Lezcano, S. Pack, C. Kanduri, M. Kanduri, V. Ginjala, A. Vostrov, et al. 2004. The binding sites for the chromatin insulator protein CTCF map to DNA methylation-free domains genome-wide. *Genome Res.* 14:1594–1602. doi:10.1101/gr.2408304

Murrell, A., S. Heeson, and W. Reik. 2004. Interaction between differentially methylated regions partitions the imprinted genes *Igf2* and *H19* into parent-specific chromatin loops. *Nat. Genet.* 36:889–893. doi:10.1038/ng1402

Ohlsson, R., R. Renkawitz, and V. Lobanenkov. 2001. CTCF is a uniquely versatile transcription regulator linked to epigenetics and disease. *Trends Genet.* 17:520–527. doi:10.1016/S0168-9525(01)02366-6

Ohlsson, R., V. Lobanenkov, and E. Klenova. 2010. Does CTCF mediate between nuclear organization and gene expression? *Bioessays*. 32:37–50. doi:10.1002/bies.200900118

Pant, V., S. Kurukuti, E. Pugacheva, S. Shamsuddin, P. Mariano, R. Renkawitz, E. Klenova, V. Lobanenkov, and R. Ohlsson. 2004. Mutation of a single CTCF target site within the *H19* imprinting control region leads to loss of *Igf2* imprinting and complex patterns of de novo methylation upon maternal inheritance. *Mol. Cell. Biol.* 24:3497–3504. doi:10.1128/MCB.24.8.3497-3504.2004

Phillips, J.E., and V.G. Corces. 2009. CTCF: master weaver of the genome. *Cell.* 137:1194–1211. doi:10.1016/j.cell.2009.06.001

Recillas-Targa, F., I.A. De La Rosa-Velázquez, E. Soto-Reyes, and L. Benítez-Bribiesca. 2006. Epigenetic boundaries of tumour suppressor gene promoters: the CTCF connection and its role in carcinogenesis. *J. Cell. Mol. Med.* 10:554–568. doi:10.1111/j.1582-4934.2006.tb00420.x

Reik, W., M. Constancia, W. Dean, K. Davies, L. Bowden, A. Murrell, R. Feil, J. Walter, and G. Kelsey. 2000. Igf2 imprinting in development and disease. *Int. J. Dev. Biol.* 44:145–150.

Renbaum, P., D. Abrahamove, A. Fainsod, G.G. Wilson, S. Rottem, and A. Razin. 1990. Cloning, characterization, and expression in *Escherichia coli* of the gene coding for the CpG DNA methylase from *Spiroplasma sp.* strain MQ1(M.SssI). *Nucleic Acids Res.* 18:1145–1152. doi:10.1093/nar/18.5.1145

Sasaki, H., K. Ishihara, and R. Kato. 2000. Mechanisms of *Igf2/H19* imprinting: DNA methylation, chromatin and long-distance gene regulation. *J. Biochem.* 127:711–715.

Schoenherr, C.J., J.M. Levorse, and S.M. Tilghman. 2003. CTCF maintains differential methylation at the *Igf2/H19* locus. *Nat. Genet.* 33:66–69. doi:10.1038/ng1057

Sparago, A., F. Cerrato, M. Vernucci, G.B. Ferrero, M.C. Silengo, and A. Riccio. 2004. Microdeletions in the human *H19* DMR result in loss of *IGF2* imprinting and Beckwith-Wiedemann syndrome. *Nat. Genet.* 36:958–960. doi:10.1038/ng1410

Srivastava, M., S. Hsieh, A. Grinberg, L. Williams-Simons, S.P. Huang, and K. Pfeifer. 2000. *H19* and *Igf2* monoallelic expression is regulated in two distinct ways by a shared cis acting regulatory region upstream of *H19*. *Genes Dev.* 14:1186–1195.

Sullivan, M.J., T. Taniguchi, A. Jhee, N. Kerr, and A.E. Reeve. 1999. Relaxation of *IGF2* imprinting in Wilms tumours associated with specific changes in *IGF2* methylation. *Oncogene.* 18:7527–7534. doi:10.1038/sj.onc.1203096

Szabó, P.E., S.H. Tang, F.J. Silva, W.M. Tsark, and J.R. Mann. 2004. Role of CTCF binding sites in the *Igf2/H19* imprinting control region. *Mol. Cell. Biol.* 24:4791–4800. doi:10.1128/MCB.24.11.4791-4800.2004

Thorvaldsen, J.L., K.L. Duran, and M.S. Bartolomei. 1998. Deletion of the *H19* differentially methylated domain results in loss of imprinted expression of *H19* and *Igf2*. *Genes Dev.* 12:3693–3702. doi:10.1101/gad.12.23.3693

Ulaner, G.A., T.H. Vu, T. Li, J.F. Hu, X.M. Yao, Y. Yang, R. Gorlick, P. Meyers, J. Healey, M. Ladanyi, and A.R. Hoffman. 2003. Loss of imprinting of *IGF2* and *H19* in osteosarcoma is accompanied by reciprocal methylation changes of a CTCF-binding site. *Hum. Mol. Genet.* 12:535–549. doi:10.1093/hmg/ddg034

Vu, T.H., A.H. Nguyen, and A.R. Hoffman. 2010. Loss of *IGF2* imprinting is associated with abrogation of long-range intrachromosomal interactions in human cancer cells. *Hum. Mol. Genet.* 19:901–919. doi:10.1093/hmg/ddp558

West, A.G., M. Gaszner, and G. Felsenfeld. 2002. Insulators: many functions, many mechanisms. *Genes Dev.* 16:271–288. doi:10.1101/gad.954702

Wolffe, A.P. 2000. Transcriptional control: imprinting insulation. *Curr. Biol.* 10:R463–R465. doi:10.1016/S0960-9822(00)00534-0

Xu, G.L., and T.H. Bestor. 1997. Cytosine methylation targetted to predetermined sequences. *Nat. Genet.* 17:376–378. doi:10.1038/ng1297-376

Yusufzai, T.M., H. Tagami, Y. Nakatani, and G. Felsenfeld. 2004. CTCF tethers an insulator to subnuclear sites, suggesting shared insulator mechanisms across species. *Mol. Cell.* 13:291–298. doi:10.1016/S1097-2765(04)00029-2